J. Phys. C: Solid State Phys. 20 (1987) 2803–2815. Printed in the UK

Stark shifts in GaAs/GaAlAs quantum wells studied by photoluminescence spectroscopy

L Viña†, E E Mendez, W I Wang, L L Chang and L Esaki
IBM Thomas J Watson Research Center, PO Box 218, Yorktown Heights, NY 10598, USA

Received 4 November 1986

Abstract. We have measured, by means of low-temperature photoluminescence spectroscopy, the dependence on the well thickness of the shift of the excitonic recombination in GaAs/GaAlAs quantum wells induced by an external electric field. With increasing thickness, up to 230 Å, an increasing Stark shift, amounting to more than 100 meV for an external field of $\sim 10^5 \mathrm{V\,cm^{-1}}$, has been found. A corresponding quenching of the luminescence intensity has also been measured. Theoretical calculations of the eigen-states have been carried out and shown to compare favourably with the experiments. Two different approaches, numerical solution of the Schrödinger equation and variational calculations of the eigen-states, yield similar results for the Stark shift. Using the latter method, the quenching of the photoluminescence is correlated with the decrease in the wavefunction overlap between electrons and holes, as they are spatially separated by the field.

1. Introduction

Since the work reported in [1] on the effects of an electric field on the luminescence of GaAs/GaAlAs quantum wells, several studies have appeared in the literature concerning the field-induced changes of the optical properties of these materials. Different techniques such as optical absorption [2–5], photocurrent spectroscopy [6–9], electroreflectance [10] and photoluminescence (PL) [6, 9, 11–13] have been employed. Two main effects have been observed, namely a Stark shift of the excitons in the wells and a concomitant quenching in the PL. Most of the measurements have been concentrated on thin wells, where the confinement effects are large, and small shifts, together with strong reduction of the PL, with increasing field, were observed. The fields have been applied not only in the longitudinal configuration (i.e. with the field perpendicular to the layers) but also in the parallel configuration [3, 5]. In the latter case, the situation is similar to that of bulk GaAs, where Stark shifts are hardly observable, because of strong lifetime reduction and impact ionisation of the excitons [14]: the excitonic resonances shift only ~10% of the excitonic binding energy before they are completely quenched. In the following, we will consider only the case of longitudinal fields, for which the heterojunction potential barriers hinder the motion of the photo-generated carriers in the direction perpendicular to the interfaces, and therefore prevent the field ionisation of the excitons [1].

† Permanent address: Instituto de Ciencia de Materiales, Universidad de Zaragoza, Consejo Superior de Investigaciones Científicas, 50009 Zaragoza, Spain.

0022-3719/87/182803 + 13 $02.50 © 1987 IOP Publishing Ltd

C18

The PL quenching was attributed to two coexisting mechanisms: spatial charge separation and field-induced tunnelling of photo-generated carriers out of the well [1, 12]. In some cases a dependence of the PL decrease on laser wavelength has been reported [12, 13], leading to the conclusion that carrier escape from the wells can account completely for this effect. Time-resolved measurements of the field-induced lifetime changes in the PL have also been performed to elucidate the importance of the different mechanisms [8, 15, 16]. A decrease of the lifetime was observed for thin wells [15, 16] (about 30–50 Å), consistent with the Fowler–Nordheim tunnelling model. This decrease is also observed when *thin* $Al_xGa_{1-x}As$ layers are used as barriers [8]. On the other hand, the opposite behaviour was obtained for wider wells [16] ($\gtrsim$100 Å), which can be satisfactorily explained by the decrease in the overlap of the electron and hole wavefunctions as they are separated by the field.

The effects of electric field on impurity-related PL have been also studied. In [11] a superlattice of wells that were 55 Å wide doped with about 4×10^{16} cm^{-3} Be was used. PL due to free and bound excitons and extrinsic $n = 1$ electrons to Be^0 acceptors near the well centre and interfaces was observed. A complicated behaviour, as a function of the external voltage, of the intrinsic and extrinsic recombination intensities was found. The extrinsic PL was enhanced at intermediate voltages, but at their highest field the intrinsic PL again dominated the spectra. No significant Stark shifts were observed in this case.

The effects of an electric field on the electronic states of QW have also been investigated theoretically by several authors [5, 17–19]. Austin and Jaros [20] extended previous calculations to consider the effects on lifetimes and spectroscopic lineshapes. They proposed an additional mechanism for the quenching of the PL, based on the broadening of the eigen-states into resonances and the corresponding decrease in the $k = 0$ component of the wavefunctions. The dissociation of excitons in QW has also been calculated [21], and found to be important only for wide wells.

The underlying motivation of these experimental and theoretical efforts is largely based on the possible use of the above-described effects to build new electro-optical devices [22]. Indeed, some applications have already been demonstrated in optical modulators [23] and bi-stable devices [24]. Recently a laser diode and a waveguide modulator have been monolithically integrated [25].

In this paper we investigate the dependence on well thickness ($2a$) of the Stark effect in $GaAs/Ga_{1-x}Al_xAs$ QWs. For small fields, a second-order perturbation calculation predicts for the energy shift of the ground state a dependence as the fourth power of the well thickness [18]. The shifts are therefore expected to increased dramatically with a. With an increase in the well thickness, the excitonic spectra of $GaAs/Ga_{1-x}Al_xAs$ resemble increasingly those of bulk GaAs. Therefore, provided the quality of the samples is good enough to provide sharp lines in the PL, the effects of the electric fields can be studied not only on free excitons but also on impurity-bound excitons. The rest of the paper is organised as follows. The experimental details are presented in § 2. A brief description of the methods used here to calculate the eigenvalues and eigen-states in a QW in the presence of a longitudinal electric field is given in §3. Section 4 deals with the experimental results, and their comparison with the calculations. Finally a discussion is presented in § 5.

2. Experiment

The samples used in our study were grown by molecular beam epitaxy on (100)-oriented

n^+-GaAs substrates. The results for three different samples with well thicknesses of 130 Å (sample A), 160 Å (sample B) and 230 Å (sample C) will be presented. In each sample, a $Ga_{0.65}Al_{0.35}As$ underlayer, with thickness ranging from 90 to 200 nm, was grown on the substrate, followed by five periods of alternate GaAs and $Ga_{0.65}Al_{0.35}As$ layers, with a barrier thickness of 25 nm. Finally, the heterostructures were capped by a 110 nm $Ga_{0.65}Al_{0.35}As$ layer. All the epitaxial materials were undoped except the first 50 nm of the $Ga_{0.65}Al_{0.35}As$ underlayer adjacent to the substrate, which were doped with Si.

An electric field perpendicular to the interfaces was applied via a semi-transparent Schottky contact formed by evaporating a Ni film on the cladding layer. The film consisted of two overlapping rectangular areas ($\simeq 1 \times 2\ mm^2$) of $\sim$100 nm and $\sim$10 nm thickness, respectively. The electrode covered only two-thirds of the total sample area, so measurements could be made by focusing the laser spot either on or off the electrode contact. A comparison, for these two situations, of the energy position and lineshape of the PL peaks provided an estimate of the flat-band condition, which corresponded to external voltages of 1.1, 0.8 and 1.02 V for samples A, B and C, respectively. This was confirmed from the small decrease in intensity and the red-shift of the PL with a further increase of the external bias, beyond the values of the built-in voltages.

The samples were mounted on TO5 headers and kept in a He-gas phase at 5 K in a variable-temperature cryostat. The QW luminescence was excited either, indirectly, with the 5145 Å line of an Ar^+ laser, above the $Ga_{0.65}Al_{0.35}As$ band-gap edge, or, selectively, with the 6471 Å line of a Kr^+ laser. The beam was focused on the thin area of the electrode on a spot 400 μm in diameter, keeping the excitation power low (ranging from 50 μW to 1mW) to avoid excessive carrier generation. The PL signal was dispersed by a $\frac{3}{4}$ m Spex double monochromator and detected with a cooled-GaAs-cathode photomultiplier. A comparison of the spectra off and on the electrode, with the samples for flat-band conditions, showed a reduction of the intensity, due to absorption in the Ni film, of one order of magnitude. Open-circuit voltages of around 0.7 V were measured under illumination with the Ar^+ laser with a power density of 150 mW cm^{-2}, while only a few mV were obtained with the Kr^+ laser under the same conditions. These small voltages indicate the nearly perfect confinement of the photo-excited carriers in the QW, when they are excited below the $Ga_{0.65}Al_{0.35}As$ band gap.

3. Theory

We will consider the case of an isolated QW in the presence of an external longitudinal electric field, using the effective-mass approximation and ignoring excitonic effects. The field-induced changes in the exciton binding energy have been discussed in the literature [5, 21] and should only amount, for the thickness of the samples used in the present work, to less than 5% of the total observed shifts [21]. We have assumed that the confined states remain quasi-bound for all fields, therefore ignoring field-induced broadening, which can contribute to the quenching of the PL [19, 20].

For a particle of mass m^* and charge e, localised in a well of width $2a$ and depth V_0, the Schrödinger equation in the presence of a longitudinal electric field, F, reads

$$-\frac{\hbar^2}{2m^*}\frac{d^2\psi}{dz^2} - (V_0 + eFz)\psi = E\psi \qquad |z| \leqslant a \qquad (1a)$$

$$-\frac{\hbar^2}{2m^*}\frac{d^2\psi}{dz^2} - eFz\psi = E\psi \qquad |z| > a \tag{1b}$$

where the origin is taken at the centre of the well.

For the calculations, the following values for the electron and heavy-hole effective masses were used: $m_E^*(\mathrm{GaAs}) = 0.067\ m_0$, $m_E^*(\mathrm{Ga_{0.65}Al_{0.35}As}) = 0.092\ m_0$, $m_H^*(\mathrm{GaAs}) = m_H^*(\mathrm{Ga_{0.65}Al_{0.35}As}) = 0.45\ m_0$, where m_0 is the free-electron mass. A 60–40% rule for the band discontinuity was chosen, leading to $V_0(\mathrm{E}) = 267$ meV and $V_0(\mathrm{H}) = 184$ meV. Two different methods were employed to solve (1) and obtain the ground states of electrons and heavy holes in the presence of the electric field.

In the first approach we have generalised the matrix formalism of [26]. The potential drop across the QW is approximated by a series of n_1 steps of width ε in the well and of n_2 steps of width η in the barrier. Typical used values are $n_1 = 80$, $n_2 = 50$, $\varepsilon = 2$ Å and $\eta = 5$ Å. In this formalism the eigenvalues of (1) are obtained by solving the equation

$$\cos kd = \tfrac{1}{2}\,\mathrm{Tr}\,\mathbf{M} \tag{2}$$

where k is the wave-vector in the well, d is the total thickness of well plus barrier and Tr represents the trace of a matrix. The matrix $\mathbf{M}$ can be written as

$$\mathbf{M} = \mathbf{A}_1\mathbf{A}_2 \ldots \mathbf{A}_n \ldots \mathbf{A}_m \tag{3}$$

where m is the total number of steps used for the potential profile ($m = n_1 + n_2$). Each of the (2×2) matrices $\mathbf{A}_n$ is obtained from the coefficients relating the continuity of the wavefunction and its derivative at the edges of the steps, and may be written as [26]

$$\mathbf{A}_n = \begin{pmatrix} \cos \alpha_n\varepsilon & (1/\alpha_n)\sin \alpha_n\varepsilon \\ -\alpha_n \sin \alpha_n\varepsilon & \cos \alpha_n\varepsilon \end{pmatrix} \qquad (E > -V_n) \tag{4a}$$

$$\mathbf{A}_n = \begin{pmatrix} \cosh \alpha_n\varepsilon & (1/\alpha_n)\sinh \alpha_n\varepsilon \\ -\alpha_n \sinh \alpha_n\varepsilon & \cosh \alpha_n\varepsilon \end{pmatrix} \qquad (E < -V_n) \tag{4b}$$

with $\alpha_n^2 = 2m^*(E + V_n)/\hbar^2$.

For the barriers, only (4b) is necessary and ε should be replaced by η. The envelope function approximation [27] is used to match the derivatives at the interfaces between GaAs and $\mathrm{Ga_{1-x}Al_xAs}$, which implies that for the potential steps $n = n_1$ and $n = m$ the second column of the matrices $\mathbf{A}_n$ are to be multiplied by the ratio

$$r = m^*(\mathrm{GaAs})/m^*(\mathrm{Ga_{1-x}Al_xAs})$$

and r^{-1}, respectively.

A variational calculation was also used to obtain the solutions of (1) and to compare the results with the method described above. To minimise the energy we used the following trial function [17]:

$$\psi(z) = \begin{cases} A \exp\left[(q_0 - \beta)\left(\dfrac{z}{2a} + \dfrac{1}{2}\right)\right] & z \leqslant -a \\ B \sin\left(k_0 \dfrac{z}{2a} + \delta\right) \exp\left(-\beta \dfrac{z}{2a}\right) & |z| \leqslant a \\ C \exp\left[-(q_0 + \beta)\left(\dfrac{z}{2a} - \dfrac{1}{2}\right)\right] & z > a \end{cases} \tag{5}$$

where β is the variational parameter. A, B and C are normalisation constants to be determined using the continuity of $\psi(z)$ and $\mathrm{d}\psi(z)/m^*(z)\,\mathrm{d}z$ at the interfaces. k_0 and q_0 are the wave-vectors of the unperturbed ground state in the well and that in the barriers, respectively, and δ is given by [27]

$$\delta = k_0/2 + \tan^{-1}(k_0/q_0). \tag{6}$$

The results of both calculations will be presented in the following section. The first approach has the advantage that it can be applied to an arbitrary potential profile and the results can be obtained by an exact numerical solution [28]. The variational calculations, on the other hand, provide easily a wavefunction that can be used to compute the overlap integral between electrons and holes, given by

$$M_{\mathrm{vc}} = \int_{-\infty}^{\infty} \psi_{\mathrm{v}}(z)\psi_{\mathrm{c}}(z)\,\mathrm{d}z \tag{7}$$

which can be compared with the integrated luminescence efficiency.

4. Results

Photoluminescence spectra of sample A (130 Å QW), at different bias voltages are shown in figure 1. These spectra were measured with the Ar^+ laser, using a power density of 150 mW cm^{-2}. Three different structures are clearly seen at the largest voltage (1.1 V), corresponding to the flat-band condition, as explained above. A comparison of the observed peak energies with envelope function calculations [27], using the parameters given in § 3, allows us to identify the different structures. The highest-energy peak (○) corresponds to the 1 E→ 1 LH exciton (E means electron and LH light hole), the high-energy line of the doublet (▼) to the 1 E→ 1 HH exciton (HH means heavy hole), and the lowest-energy peak (●) to a donor-bound exciton (D, X). The last assignment is based on the rapid decrease of this structure as the temperature is increased above about 12 K, its saturation as the laser power density is increased, and its energy difference with the free exciton (≃1.2 meV), similar to the corresponding difference in bulk GaAs.

As the external voltage is decreased (i.e., the electric field is increased) a strong quenching of the LH exciton is observed, so it could be followed only to −0.3 V. A relatively complicated behaviour of the free HH and (D, X) excitons is seen with increasing field. Down to voltages of about −0.9 V the free exciton decreases rapidly, with a corresponding increase of the bound exciton. The total integrated intensity remains roughly constant down to about −0.3 V and then decreases monotonically. For voltages smaller than −1 V the free exciton dominates again over the bound exciton, as can be seen by comparing the spectra at −1 and −1.1 V. This behaviour is similar to that observed in p-doped QWs [11]. The increasing broadening of the PL with increasing field prevents us from resolving the two structures for voltages smaller than −2 V, although both are believed to remain in the spectra, by analogy with the behaviour of similar samples.

The inset in this figure shows the energy thresholds of the three excitons as a function of external bias, down to voltages where the free HH and (D, X) excitons could be resolved separately. The energy difference between these two structures remains constant for all applied voltages, indicating that the changes of the binding energies of free and bound excitons with electric field are the same. The LH exciton also shifts, with a

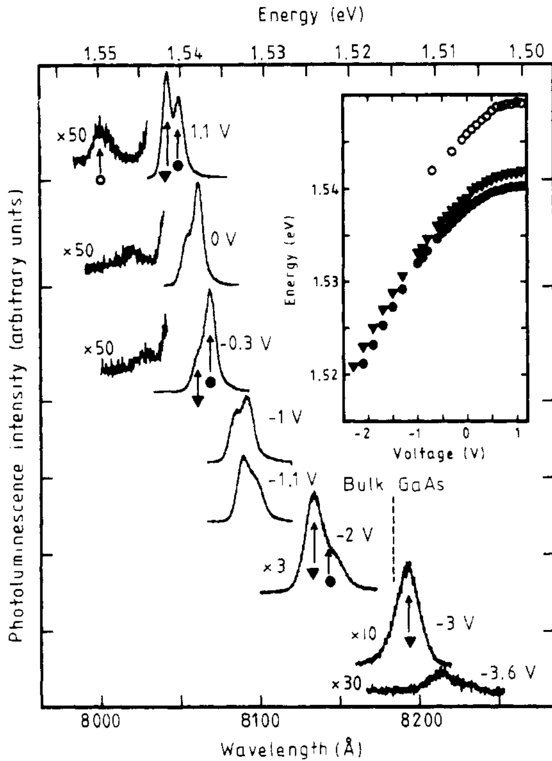

Figure 1. Photoluminescence spectra of sample A (130 Å QW) at different external bias voltages. Scaling factors are indicated on the LHS of the spectra (when no factor is given, × 1 is assumed). The total applied voltage through the sample is indicated on the RHS. The free LH, HH and donor-bound excitons are marked with ○, ▼ and ●, respectively. The spectra are displaced vertically for clarity. The vertical broken line depicts the energy of the bulk GaAs free exciton. The inset shows the energy thresholds of the three structures in the range of coexistence.

similar rate to that for the HH exciton. The slightly larger shift, apparent in the figure, was neither observed in other samples nor in photocurrent measurements of these samples [29]; it may well arise from uncertainties in the assignment of the peak positions in this weak structure.

Figure 2 displays the PL spectra between 0.8 and −2.5 V for sample B (QW 160 Å thick). Similarly to the case for sample A, three different structures can be observed for the flat band (0.8 V), which correspond, with decreasing energy, to the free LH (○), free HH (▼) and (D, X) (●) excitons. The same laser line and power density as for sample A were used in this case. The rate of decrease of the LH exciton intensity is again much larger than that of the HH, and could only be traced down to 0.3 V. In this case the bound exciton also weakens rapidly and becomes submerged with the free-HH exciton at high fields, giving rise to the apparent increase in the linewidth. The inset in this figure shows the energy thresholds of the three excitons for voltages where all the structures could be resolved separately. One observes again a parallel shift, within experimental error, of all the excitonic structure.

Spectra corresponding to sample C (230 Å QW), measured at 80 mW cm^{-2}, are depicted in figure 3. In this case the LH exciton, observable only at flat-band conditions

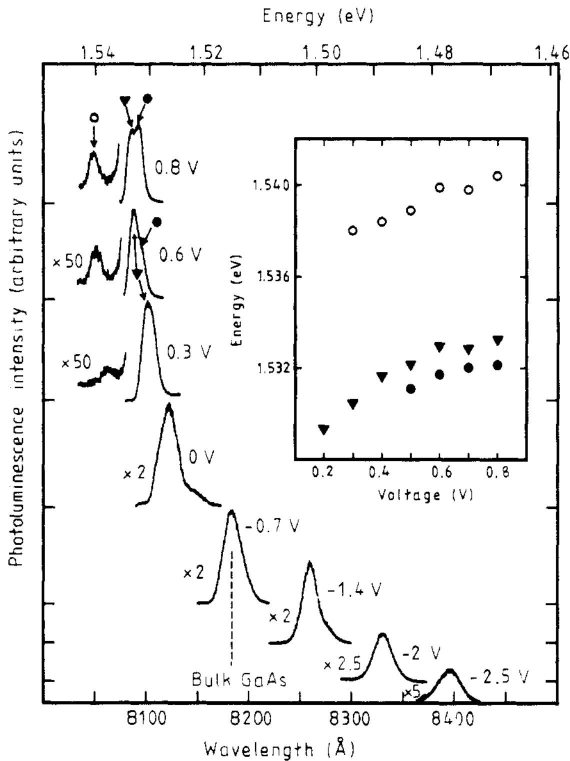

Figure 2. Photoluminescence spectra of sample B (160 Å QW) for different external voltages; the symbols have the same meaning as in figure 1. Peak energies, in the region where all structures could be resolved separately, are shown in the inset.

($\simeq$1 V), is not shown in the figure. We assign the structures at the two larger voltages to free HH (▼) and (D, X) (●) excitons. The small shoulder seen on the low-energy side is due to the PL of the heavily doped GaAs substrate. A decrease of the external voltage reduces the free-exciton peak strongly, which can be seen only as a shoulder in the spectrum at 0.8 V. A further decrease of the bias voltage produces a quenching of the (D, X) exciton but simultaneously makes resolvable a third structure (see the spectrum at 0.4 V). The energy difference between this new structure (■) and (D, X) is about 1.6 meV. We tentatively assign this structure, which is the only one that remains visible below −0.5 V, to an acceptor-bound exciton (A,X). The energies of the three structures are plotted as functions of the external voltage, in the range from 1 to −0.5 V, in the inset of the figure. They shift parallel to each other, as in the cases of thinner wells.

The Stark shifts of the dominant peak for the three samples are plotted in figure 4 versus the electric field strength. The zero in the field scale corresponds to flat-band conditions, estimated as described previously. For the QW 130 Å thick, for example, a small downward shift can be seen below zero field when the applied external voltage is beyond the flat band. The expected increasing shift with increasing well thickness, for the same electric field, is clearly observed in this figure. Shifts as large as 32, 60 and 100 meV, for around 1×10^5 V cm^{-1}, are obtained for the wells with widths 130, 160 and 230 Å, respectively. This causes the excitonic recombination to evolve below the bulk GaAs exciton for these relatively thick wells (the energy corresponding to the bulk

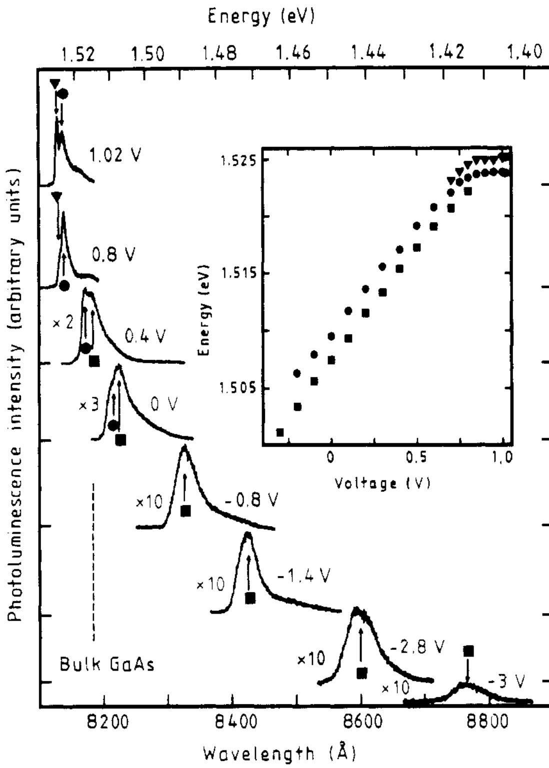

Figure 3. The excitonic photoluminescence of sample C (230 Å QW). Free HH, and donor- and acceptor-bound excitons are marked with ▼, ●, and ■, respectively. Note the large shift (about 100 meV) of the PL below the band gap of bulk GaAs. The inset shows the peak positions as a function of applied voltage, in the range of coexistence of all structures.

GaAs exciton is indicated in the figure by a broken curve). The results of the calculations obtained using the parameters given in § 3 are also summarised in figure 4. The full curves represent the exact numerical solution obtained using the matrix formalism and the broken curves correspond to the variational procedure.

Finally, the decrease of the integrated PL intensity (●), for sample B, is plotted in figure 5 versus electric field strength. The change of the overlap integral (M^2_{vc}), obtained from the variational calculation, is shown in this figure as a full curve.

5. Discussion

The results of the two kinds of calculations for the HH exciton are compared in figure 4, together with the experimental shifts. The curves are obtained by adding the GaAs band gap to the calculated energies of the electrons and holes in the wells and subtracting the two-dimensional exciton binding energy, which we have assumed to be independent of field. For this purpose, binding energies of 8, 7 and 6 meV [30] were used for samples A, B and C, respectively. Using the fact that for fields where free and bound excitons coexist, they shift parallel to each other, we have compared, for sample C, the calculations with the shift of the (A, X) exciton (this structure was the only one resolvable

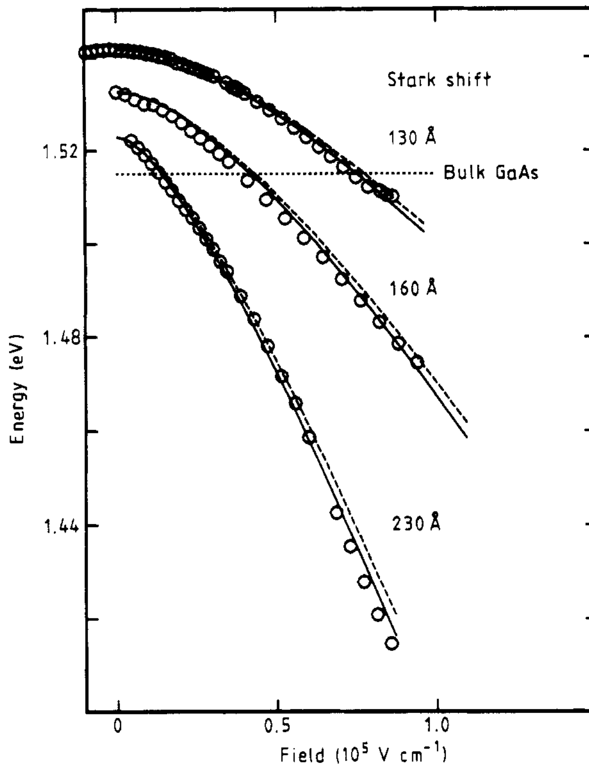

Figure 4. Circles: experimental free-exciton energies as a function of electric field strength for samples A and B. In the case of sample C (230 Å), the experimental points correspond to the acceptor-bound exciton. Full and broken curves: theoretical shift obtained with numerical calculations, using the matrix formalism described in the text, and variational results, respectively. The horizontal dotted line indicates the energy of the free exciton in bulk GaAs.

at high fields). The observed energy difference between the free exciton and (A, X), 5 meV, was in this case also subtracted from the theoretical results.

The two calculations are in good agreement at low fields. At high fields, slightly smaller shifts are obtained in the variational calculation than in the numerical results. The largest deviation amounts, however, to only 4% at the highest experimental field. In both calculations the effect of the field is more pronounced for holes than for electrons (their relative contributions are not shown here), due to heavier effective mass and the lower barrier for the holes. The agreement between the theory and the experiment is quite satisfactory, with an uncertainty of about 10%, from the following considerations. The fields shown in figures 4 and 6 are averaged fields, taken as the ratio of the applied external voltage to the total thickness of the layers grown on the n^+-GaAs substrate. The width of the GaAs wells can be determined with reasonable accuracy by comparing the exciton energies, measured without an electric field, with calculations of the electron and hole ground states in a finite well. The main uncertainty lies in the widths of the thick $Ga_{0.65}Al_{0.35}As$ cladding layers. From growth parameters, the total thickness of $Ga_{0.65}Al_{0.35}As$, including cladding and barrier layers, is estimated to be 410 (sample A), 290 (sample B) and 360 nm (sample C). We have allowed for a 10% uncertainty in these thicknesses, and scaled the averaged field between these limits so as to obtain the best fit of the calculations to the experimental results.

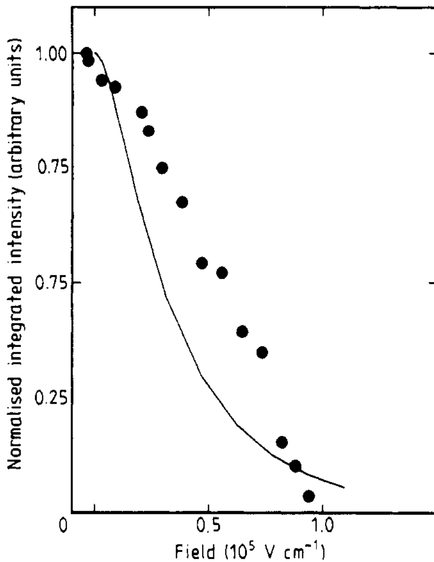

Figure 5. The integrated photoluminescence intensity versus electric field, normalised with respect to flat-band conditions, for sample B (160 Å QW). The full curve depicts the change in the overlap between electron and hole wavefunctions.

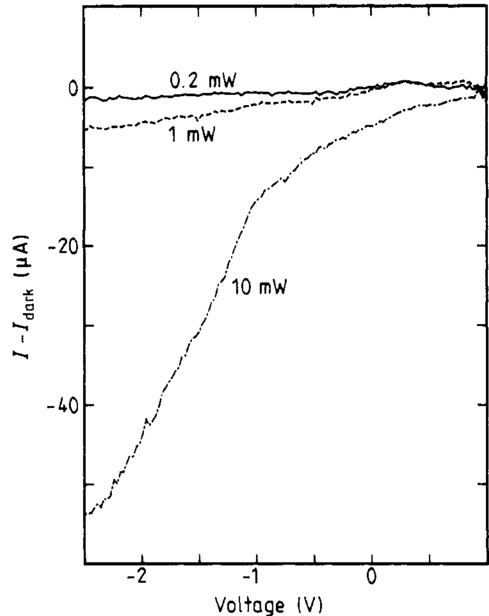

Figure 6. The increase in reverse-bias current with Ar$^+$-laser illumination (160 Å QW), with respect to the dark current, for several excitation powers. 1 mW was the highest power used in the PL experiments; the 10 mW curve is shown only for comparison.

Field-induced quenching of the photoluminescence has been observed by several authors [1, 6, 8, 12, 31]. Different mechanisms, such as decrease of the oscillator strength and increase of non-radiative processes, have been proposed to account for the observed decrease in PL efficiency. The field-induced polarisation of the electron and hole wavefunctions in opposite directions in the QW results in a decrease of the overlap integral M^2_{vc}, and thus a decrease in the oscillator strength and the PL intensity. For thin wells [1, 15], the magnitude of this effect was found to be too small to explain the observed PL quenching. Tunnelling of carriers out of the QW was assumed to be the most important mechanism in this case. With excitation above the $Ga_{1-x}Al_xAs$ band gap, a large increase in the photocurrent ($\simeq$500 μA), together with a strong quenching of the PL has been reported in [12, 13] for two samples, one of them consisting of a single 50 Å QW, and the second containing three isolated wells of 50, 75 and 100 Å. They concluded that the PL quenching in QWs was caused by the leakage of photo-generated carriers through the barriers rather than by an increase of non-radiative processes or a decrease of the overlap between electron and hole wavefunctions. The use of *thin* $Al_xGa_{1-x}As$ layers as barriers for the wells also enhances the tunnelling mechanism [8].

Recently, time-resolved photoluminescence measurements [16] have shown that, for samples where non-radiative processes are negligible, no quenching of the photoluminescence is observed and an increase of the radiative lifetime with increasing electric field is obtained. The luminescence efficiency can be written as:

$$\eta = 1/(1 + \tau_{\text{radiative}}/\tau_{\text{non-radiative}}). \tag{8}$$

If the non-radiative processes are negligible ($\tau_{\text{non-radiative}}$ much larger than $\tau_{\text{radiative}}$), then an increase of the radiative lifetime will not affect the luminescence efficiency, in agreement with the measurements in [16]. On the other hand, experimental evidence of an increase in the radiative lifetime together with a decrease of the luminescence intensity has been found for a well 120 Å thick [31]. Calculations of the field-induced changes of the oscillator strength could explain the increase in the radiative lifetime and the luminescence quenching [16, 31].

Our data in figures 1–3 show a quenching of the luminescence by one order of magnitude, therefore indicating that non-radiative channels are present in our samples. The contribution of Fowler–Nordheim tunnelling can be obtained from photocurrent measurements [12]. We show in figure 6 the increase in the photocurrent under illumination with respect to the dark current versus applied voltage. The measurements were performed at 5 K under excitation with the 5145 Å line of the Ar^+ laser. This figure can be compared with figure 2(*a*) of [12]. For the highest excitation power used in our PL measurements (1 mW) only a slight increase in the reverse current (5 μA) is observed at the largest negative-bias voltage. For comparison we also show data taken at 10 mW, a power one order of magnitude higher than that used for PL; even at this high level of excitation, the current increase amounts to only about 50 μA. Similar results were obtained for the two other samples investigated here, thus demonstrating that for thick ($\geqslant$100 Å) wells tunnelling can be ruled out as an important mechanism, at moderate fields, for the PL quenching. PL lifetime measurements [15, 16] also indicate the existence of two different regimes: for thin wells a decrease of the lifetime has been measured [15, 16], pointing to an increase of Fowler–Nordheim tunnelling, while for thick wells, the observed increase in PL lifetime could be understood on the basis of an increase in the spatial separation of electrons and holes with increasing field [16, 31].

Our measurements do not allow us to discern between the two other possible mechanisms responsible for the quenching of the luminescence. Either a decrease of the non-radiative recombination lifetime ($\tau_{\text{non-radiative}}$ in (8)) or an increase in $\tau_{\text{radiative}}$ can produce the observed decrease in the luminescence efficiency. Our data in figure 5 show, however, a reasonable agreement between the experimental quenching of the PL and the decrease in the overlap integral M_{vc}^2 with increasing field (similar qualitative agreement was obtained for samples A and C). This agreement favours the interpretation of the decrease in the oscillator strength as the main mechanism for the luminescence quenching in thick quantum wells. At large fields, the rate of increase of charge polarisation becomes smaller, because the carriers are skewed into quasi-triangular wells on each side of the QW (note the saturation of the full curve in figure 5). The observed further quenching of the PL is likely to be caused by the sweeping of the carriers out of the QW.

We believe that two different regimes have to be distinguished: for thin wells ($2a \leqslant 100$ Å) the confinement energy is large; thus the effective tunnel barrier for the carriers is small, and Fowler–Nordheim tunnelling of the carriers out of the QW will probably play a dominant role in the PL quenching. On the other hand, for thick wells, this process becomes less probable and will not be important until very high fields are applied.

With increasing QW width, the PL spectra increasingly resemble those of bulk GaAs, where, generally, bound excitons dominate over free excitons. The spectra, particularly those of sample C in figure 3, show clearly the bound-exciton recombination as the external voltage is decreased. The phenomenon of field-enhanced bound exciton actually occurred even for thinner wells [9]. We attribute this enhancement again to the polarisation of the electron and hole wavefunctions toward the interfaces, where more

impurities tend to accumulate. The predicted maxima in the density of impurity states in the vicinity of the edges of the well [30, 32] also favour this explanation. Consistent with this notion is the dominance of the (A, X) recombination in the PL lineshape, at high fields, as the shift of the holes toward the edges of the well is faster than that of the electrons, because of the smaller valence-band-edge discontinuity and the larger HH effective mass [17].

It is also very interesting to note that for such a wide well (230 Å), almost comparable to the three-dimensional exciton diameter (≃300 Å), the electron–hole interaction remains strong at high fields, and excitons still exist when the Stark shift considerably exceeds the exciton binding energy. Evidently, even for wide wells, impact ionisation is not an important mechanism for the quenching of the PL.

A faster quenching of the LH exciton relative to the HH exciton is observed in figures 1 and 2. This is different from our calculations which predict a comparable or even a slightly smaller decrease in the wavefunction overlap for LH than for HH. The explanation may lie in additional effects, such as the decrease of the binding energy, and in the rate of sweep-out of the holes in the QW, both of which have been predicted to be larger for the LH than for the HH [21], under electric fields.

We would like to remark that, for the three samples measured, large Stark shifts of the electron and hole eigen-states give rise to PL below the band gap of bulk GaAs. The carrier recombination is indirect in real space, as the electrons and holes are skewed in opposite directions and are confined in quasi-triangular wells close to the interfaces.

Finally, we would like to comment on the occasional presence of a small non-shifting peak, at the photon energy corresponding to the free HH exciton at flat band. Non-shifting peaks, accompanying other shifting structures, have also been reported in the literature [13], and these have been interpreted [13] as a competition between two processes, intrinsic free-exciton recombination and recombination between the $n = 1$ electrons and neutral acceptor centres. The shift was attributed to an enhancement of the extrinsic PL as the electrons and holes are skewed by the electric field toward the interfaces, while both intrinsic and extrinsic PL remained at the same energy. However, no explanation was given of the fact that only the wavefunctions were affected by the field without any change in the energy values.

A close examination of our measurements showed that this non-shifting peak, constant in intensity, was caused by indirect excitation of the uncovered area of the sample, i.e. by scattered light reflected in the windows or somewhere else in the cryostat. This spurious structure was eliminated from the spectra, in our case, by careful coverage of the exposed area of the sample.

6. Conclusions

We have measured the thickness dependence of the Stark effect in wide (>100 Å) GaAs–$Ga_{1-x}Al_xAs$ quantum wells. A large increase in the field-induced red-shifts with increasing thickness, as predicted by simple second-order perturbation theory arguments, has been found. A reasonable agreement between our calculations and the experimental results have been obtained, within a 10% uncertainty, due to growth parameter determination. For the range of well thickness used in our experiments, a satisfactory agreement between the observed quenching of the PL and the theoretical predictions of variational calculations has been obtained. The enhancement of the bound-exciton luminescence at high fields has been interpreted as a result of the spatial

separation of carriers towards the heterojunction interfaces, where more impurities exist.

Acknowledgments

We would like to thank L Alexander for his assistance in sample preparation, and R T Collins for many helpful discussions. One of the authors (LV) would like to thank the Max-Planck Society (Federal Republic of Germany) for a fellowship. This work was sponsored in part by the US Army Research Office.

References

[1] Mendez E E, Bastard G, Chang L L, Esaki L, Morkoc H and Fischer R 1982 *Phys. Rev.* B **26** 7101; 1983 *Physica* B **117+118** 711
[2] Chemla D S, Damen T C, Miller D A B, Gossard A C and Wiegmann W 1983 *Appl. Phys. Lett.* **42** 864
Wood T H, Burrus C A, Miller D A B, Chemla D S, Damen T C, Gossard A C and Wiegmann W 1984 *Appl. Phys. Lett.* **44** 16
[3] Miller D A B, Chemla D S, Damen T C, Gossard A C, Wiegmann W, Wood T H and Burrus C A 1984 *Phys. Rev. Lett.* **53** 2173
[4] Iwamura H, Saku T and Okamoto H 1985 *Japan. J. Appl. Phys.* **24** 104
[5] Miller D A B, Chemla D S, Damen T C, Gossard A C, Wiegmann W, Wood T H and Burrus C A 1985 *Phys. Rev.* B **32** 1043
[6] Polland H J, Horikoshi Y, Höger R, Göbel E O, Kuhl J and Ploog K 1985 *Physica* B **134** 412; 1986 *Surf. Sci.* **174** 278
[7] Collins R T, von Klitzing K and Ploog K 1986 *Phys. Rev.* B **33** 4378
[8] Masumoto Y, Tarucha S and Okamoto H 1986 *Phys. Rev.* B **33** 5961
[9] Viña L, Collins R T, Mendez E E and Wang W I 1986 *Phys. Rev.* B **33** 5939
[10] Alibert C, Gaillard S, Brum J A, Bastard G, Frijlink P and Erman M 1985 *Solid State Commun.* **53** 457
[11] Miller R C and Gossard A C 1983 *Appl. Phys. Lett.* **43** 943
[12] Horikoshi Y, Fischer A and Ploog K 1985 *Phys. Rev.* B **31** 7859
[13] Horikoshi Y, Fischer A and Ploog K 1985 *Japan. J. Appl. Phys.* **24** 955
[14] Bludau W and Wagner E 1976 *Phys. Rev.* B **13** 5410
[15] Kash J A, Mendez E E and Morkoc H 1985 *Appl. Phys. Lett.* **46** 173
[16] Polland H J, Schultheis L, Kuhl J, Göbel E O and Tu C W 1985 *Phys. Rev. Lett.* **55** 2610
[17] Bastard G, Mendez E E, Chang L L and Esaki L 1983 *Phys. Rev.* B **28** 3241
[18] Fernandez F M and Castro E A 1982 *Physica* A **11** 334
[19] Austin E J and Jaros M 1985 *Phys. Rev.* B **31** 5569
[20] Austin E J and Jaros M 1985 *Appl. Phys. Lett.* **47** 274; 1985 *J. Phys. C: Solid State Phys.* **18** L1091
[21] Brum J A and Bastard G 1985 *Phys. Rev.* B **31** 3893
[22] Yamanishi M and Suemune I 1983 *Japan. J. Appl. Phys.* **22** L22
[23] Wood T H, Burrus C A, Miller D A B, Chemla D S, Damen T C, Gossard A C and Wiegmann W 1985 *IEEE J. Quantum. Electron.* **QE-21** 117
[24] Miller D A B, Chemla D S, Damen T C, Gossard A C, Wiegmann W, Wood T H and Burrus C A 1984 *Appl. Phys. Lett.* **45** 13
[25] Tarucha S and Okamoto H 1986 *Appl. Phys. Lett.* **48** 1
[26] Smith R A 1969 *Wave Mechanics of Crystalline Solids* (London: Chapman and Hall) ch 4
[27] Bastard G 1981 *Phys. Rev.* B **24** 5693
[28] Mendez E E and Viña L unpublished
[29] Collins R T, Viña L, Mendez E E and Wang W I unpublished
[30] Bastard G 1981 *Phys. Rev.* B **24** 4714
[31] Kan Y, Yamanishi M, Usami Y and Suemune I 1986 *IEEE J. Quantum. Electron.* **QE-22** 1837
[32] Bastard G, Mendez E E, Chang L L and Esaki L 1983 *Solid State Commun.* **45** 367